scientific reports

Check for updates

OPEN

Human mobility in the metaverse mirrors patterns in the physical world

Kishore Vasan[1], Márton Karsai[2,3] & Albert-László Barabási[1,2,4]✉

The metaverse is a virtual space enabling interactions beyond geographical boundaries, promising to transform how people engage with each other both in the digital and the physical worlds. The lack of geographical boundaries and travel costs in the metaverse prompts us to ask if the fundamental laws that govern human mobility in the physical world apply. We collected data on avatar movements from Decentraland, along with their network mobility extracted from NFT purchases on Ethereum and Polygon. We find that despite the absence of mobility costs, an individual's inclination to visit new locations diminishes over time, limiting movement to a small fraction of the metaverse. We also find a lack of correlation between land prices and visitation, a deviation from the patterns characterizing the physical world. Finally, we identify the scaling laws that characterize meta mobility and show that we need to add preferential selection to the existing models to explain quantitative patterns of metaverse mobility. Our ability to predict the characteristics of the emerging meta mobility network implies that the laws governing human mobility are rooted in fundamental patterns of human dynamics, rather than the nature of space and cost of movement.

The metaverse is an interoperable virtual ecosystem that merges augmented and virtual reality, artificial intelligence, and blockchain technologies to create immersive, interactive, and persistent digital experiences[1]. Unlike traditional online gaming platforms, it is built on decentralized principles that enable new forms of participation in virtual economies and foster novel modes of humans interactions on the internet[2–4]. For example, asset ownership and verification on the popular metaverse *Decentraland* are managed through Non-Fungible Tokens (NFT)[5,6], setting it apart from closed, centrally controlled gaming ecosystems like Minecraft[7]. Driven by the potential of the technology and its far-reaching impact on society, in 2022, metaverse companies attracted over $120 billion in investments[8].

Historically, human movements are confined to the tangible realm of the physical world, limited by structural and natural boundaries, and the time and cost associated with mobility. Facilitated by detailed data on individual human movements, studies have revealed the existence of multiple universal laws and patterns governing human mobility[9–11], and have inspired the development of a family of quantitative models capable of explaining these patterns[12,13]. The resulting modeling framework quantifies the balance of physical proximity and economic prospects in shaping human mobility[14,15], and its impact on socio-economic segregation[16–19]. This rich body of literature probes human behavior patterns, and have pledged a leading role during the COVID-19 pandemic, when mobility-based approaches were indispensable in predicting the spread of the pathogen, and have fueled contact tracing algorithms[20–23].

A distinguishing feature of the metaverse is that individuals are no longer limited by geographic constraints or by the expenses and time investment associated with travel, allowing them to seamlessly transition between different locations[24]. In this new multi-dimensional landscape, traditional modeling frameworks inspired by transportation modes and residential choices[25], opportunities and geographical restrictions deeply rooted in the physical space of human existence[26,27], may no longer apply. Therefore, we need to ask whether the well-established laws and patterns governing human mobility continue to apply, and if not, how do we develop a new modeling framework for the virtual space, where choices are driven by individual preferences, popularity, and network effects, rather than physical distance.

Prior research on virtual ecosystems has identified regularities in human behavior, such as the influence of social network structures in determining user exploration trajectories[28,29], and its implications on economic activities such as location prices in the virtual world[30,31]. In the context of web exploration, studies have shown

[1]Network Science Institute, Northeastern University, Boston, Massachusetts, US. [2]Department of Network and Data Science, Central European University, Vienna, Austria. [3]HUN-REN Alfréd Rényi Institute of Mathematics, Budapest, Hungary. [4] Channing Division of Network Medicine, Harvard Medical School, Boston, Massachusetts, US. ✉email: barabasi@gmail.com

that individual preferences closely mirror real-world exploration behavior[32–34]. In contrast to previous studies that investigated mobility on the internet[35,36], we develop foundational principles within the context of the metaverse, and relate these findings to physical mobility models. Importantly, we track individual movements at ten-second intervals within a large-scale virtual world and directly linking these trajectories to blockchain-based NFT transactions, offering fine-grained data on individual patterns. This data-driven approach provides a fresh perspective on the interplay between spatial mobility, social interactions, and economic activities within a unified analytical framework.

We focus on public data collected from two separate metaverse systems: (a) The first captures individual movements within a two-dimensional (2D) virtual environment. As the movements are confined to a pre-defined grid, it offers an environment whose metrics are comparable to the physical world. (b) The second data focuses on contract mobility, capturing the movement of the individuals observed in (a) across different blockchain-based NFT contracts. This data describes mobility in an infinite dimensional space, where movements are not limited by an explicit physical boundary. Importantly, the data collection effort enables us to track the mobility of the *same individuals* across both blockchain-driven systems, ultimately offering a comprehensive and novel perspective on human behavior within the metaverse ecosystem (Fig. 1 A).

Our results indicate that despite the absence of mobility costs, an individual's inclination to explore new locations diminishes over time. As a result, movement is heavily concentrated in a few locations in the metaverse, resulting in a pronounced disparity in visitor distribution across various locations. Importantly, we find a lack of correlation between land prices and visitation, underscoring the distinctive feature of the metaverse, where economic and spatial mobility dynamics deviate from the persistent patterns identified in the physical world. Finally, we show that to explain the observed metaverse mobility patterns and the emerging scaling laws, we need to modify the prevailing mobility models, incorporating a preferential selection mechanism for location selection. The proposed modification, a meta-mobility model called *m-EPR*, predicts mobility network and heterogeneous mobility flows in line with the empirically observed features in the metaverse. The ability of the *m-EPR* model to accurately describe the mobility network implies that individual movement in the metaverse is driven by popularity-based dynamics, a feature absent from human mobility in the physical world.

Data collection and curation

Virtual world mobility. To examine mobility in the metaverse we focused on Decentraland, one of the first decentralized virtual worlds launched in 2019 (Fig. 1 B), featuring 90,601 distinct lands (locations), each of size 16 by 16 meters in the virtual space and organized in a symmetrical layout. Decentraland offers the opportunity to explore mobility in the three-dimensional space and relate the movement to ownership structures. As the locations are mapped using NFTs on the Ethereum blockchain, we track individual ownership and analyze the trends in the price changes (Supplementary Section 1.2). We collected temporal mobility data of users on the platform in two separate sessions: from March 15, 2022 to August 7, 2022 (D1) and from August 8, 2022 to September 19, 2022 (D2), together capturing information on 163,770 users and their 251,643,262 movements. The two data sources (D1 and D2) only differ on the servers used to collect the data and capture identical mobility data structures, hence we present the results on the combined data (Supplementary Section 1). Using this data, we build a virtual world mobility network, where nodes are locations and a link signifies movement across the two locations.

Network mobility. Every NFT purchase is publicly documented on the blockchain, establishing a fail-proof system of verifiable ownership. On the blockchain, this is primarily done using ERC-721 contracts, an Ethereum protocol used to represent and transfer digital assets. Focusing on the set of 163,770 individuals whose mobility we tracked on Decentraland, we extracted their network mobility by collecting data regarding their NFT purchases from two blockchains: (a) *Ethereum*, finding 1,165,310 NFTs from 23,827 contracts collected by 14,732 (9%) users, and (b) *Polygon*, finding 3,112,300 NFTs from 54,918 contracts engaging 41,870 (25%) users. Using this data, we construct a dynamic network in which nodes represent NFT contracts (locations) and links capture time-resolved purchase patterns between those contracts (Fig. 1 C). In particular, we track each user's exploration trajectory and define links between contracts based on sequential movements. For example, a link between contracts C1 and C2 is formed when a user purchases a NFT from contract C1 at time t and then proceeds to purchase a NFT from contract C2 at time $t+1$. This procedure reveals meaningful connections and emergent structure of the contract network for analysis and modeling.

The decentralized software architecture of the Decentraland metaverse and the transparent nature of blockchain technology allows us to collect data about individual behavior, making it a viable and suitable source for scientific studies. While it does not contain privately identifiable information, the psuedo-anonymous nature of blockchain transactions could contain the risk of de-anonymization since it can be linked to a natural person identity, as noted by the European Union General Data Protection Regulation[37]. Given this, we secured the necessary approval from the Institutional Review Board (IRB) for our study (Reference number 23-03-29).

Results

Characterizing individual movements

The movement of individuals in the physical world are guided by established patterns of regularity, shaped by the location of home and workplace, and the physical distances between them[38,39]. The design of these factors have lead to the development of statistical models that predict individual mobility[9]. In the metaverse, the absence of traditional points of interest and mobility costs prompts us to ask: do individuals typically explore a significant portion of the available locations? Importantly, do the principles that govern individual mobility in the physical world hold true within the metaverse?

To answer this, we first measure the number of unique locations visited by an individual. We find that a typical individual explored 18 locations (lands) within the virtual world, or less than 1% of all lands (Supplementary

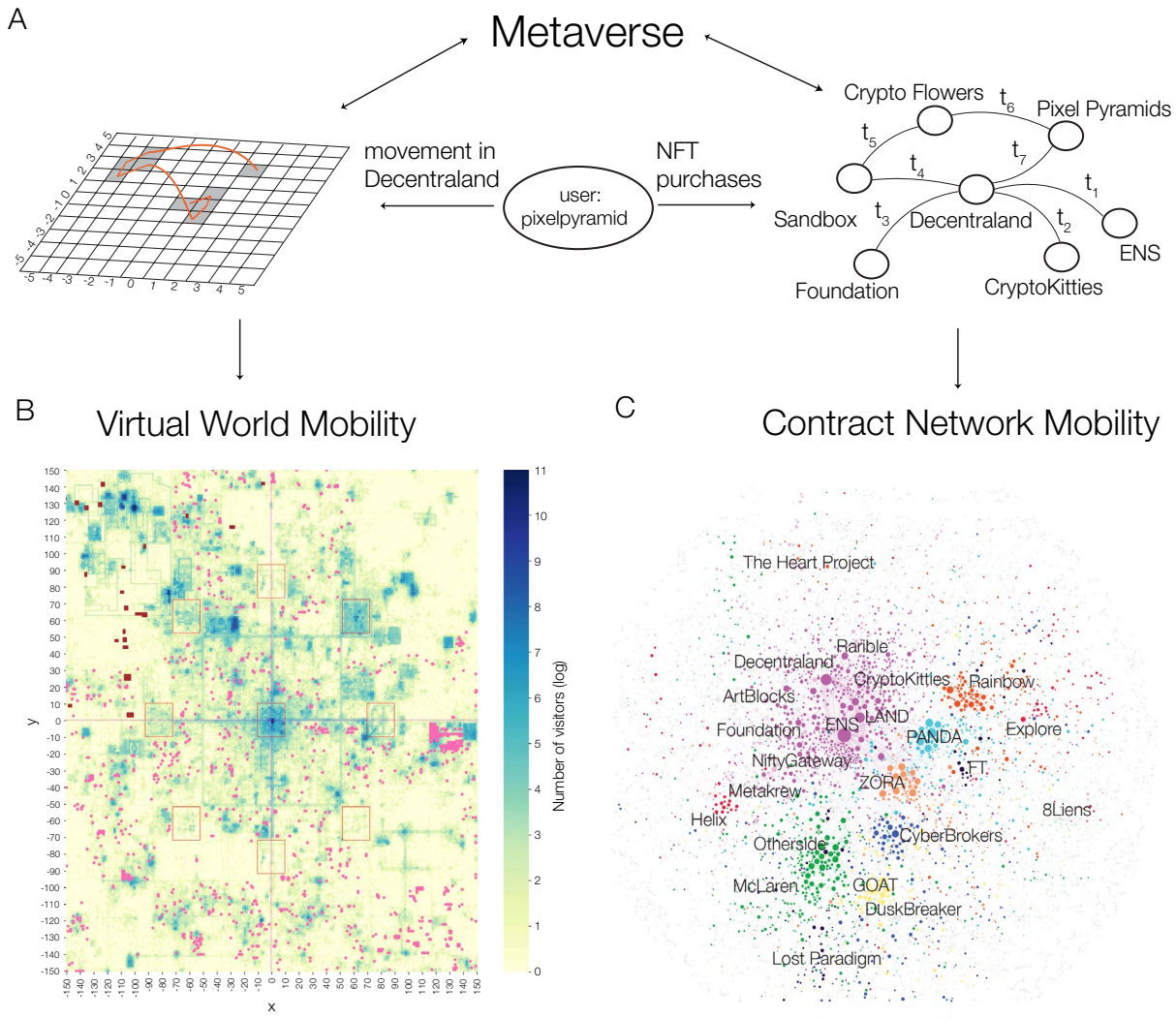

Fig. 1. Measuring meta-mobility. **(A)** To quantify mobility in the metaverse, we explore two separate datasets: Mobility in a 2-dimensional virtual world (left) and in the network space (right). In the virtual world, an individual, posing as an avatar, can move through a 2D virtual environment via local movements or teleportation. Using the trajectories of all individuals in the virtual world, we created a mobility network, whose nodes are lands and a link captures the movement between two locations. We track the mobility of the same individuals in the network space, capturing virtual marketplaces through their NFT purchases, allowing us to build a time-resolved contract network. For example, a user with screen name *pikelpyramid*, purchased an NFT from the *Decentraland* contract and the subsequently purchased a new NFT from *Sandbox*, creating a link between *Decentraland* and *Sandbox*. **(B)** Visualization of the Decentraland virtual world. Each land in the virtual world is identified by its (x, y) coordinates, organized in a 2D symmetrical layout. The lands are colored based on the number of visitors. We mark the parcels that were sold during our observation period, with points sized based on the selling price of land. **(C)** The Ethereum contract network traveled by our users. The nodes (contracts) are sized based on the number of users that visit the contract, and the top 10 network communities are colored for clarity.

Figure S10 A). The most active participant visited 2,973 locations, corresponding to 3.2% of the exploration space. Further, individuals who owned virtual land or digital currency in the metaverse explored an average 39 locations, whereas those without any financial involvement explored only 14 locations on average. In a similar fashion, an average user bought NFTs from 20 different contracts on Ethereum, representing less than 0.1% of all contracts, and an average user on Polygon purchased from 8 contracts, representing less than 0.1% of all contracts (Supplementary Fig. S10 B). These patterns suggest that despite the lack of physical and time restrictions to discover and explore new locations, individuals tend to focus their mobility to a small fraction of the metaverse.

To study the role of displacements in the metaverse, we next quantify the jump distance, δ_r. In the virtual world, we can rely on the Manhattan distance, where a distance of five indicates displacement to a land located five units away in any direction (Fig. 1 B, Supplementary Fig. S12, Supplementary Section 3). We find that individuals continue to prefer to move in smaller distances and rarely display large displacements (Fig. 2 C).

Specifically, jumps greater than a distance of ten accounts for only 18% of all displacements (Supplementary Fig. S13). In contrast to the physical world where the distance between two locations can be used to predict visitation frequency (25,34,40), in the virtual world spatial separation between locations does not affect an individuals likelihood to visit a location (Supplementary Fig. S14).

In the contract mobility space, distance is measured using the shortest path length between the two contracts (locations) on the contract network (Fig. 1 C). Similar to the mobility patterns in the virtual world, we find that individuals prefer to purchase from contracts within one to three steps in the contract network (Fig. 2 D). Furthermore, individuals tend to repeatedly return to the same contract: we observe a 63% retention rate on Ethereum, and a 82% retention rate on Polygon, suggesting a "lock-in" effect in the metaverse, similar to the patterns found in web browsing[41].

To characterize the variability in time allocation across locations, we employ two metrics: the mean visitation frequency of each individual, $f_i = n_i/S_i$, where n_i is the total time spent and S_i is the number of unique locations visited by individual *i*, and the total dispersion in visitation across all locations, σ_{f_i}, allowing us to assess the degree of heterogeneity in how individuals allocate their time across different locations. We find that the visitation flux in the metaverse follows the scaling law $\sigma_f \propto \langle f \rangle^{\beta}$, where the exponent in the virtual world is $\beta_{vw} = 1.01$ (Fig. 2 E), and in the network space it follows $\beta_{ethereum} = 1.01$ and $\beta_{polygon} = 0.98$ (Fig. 2 F). The observed $\beta \sim 1$, indicates that as individuals explore more locations, the variability of their interests also grows linearly.

We examined the location discovery rate of individuals, quantified as the number of unique locations visited, *S*(*n*), after *n* movements. We find that the exploration patterns of individuals follows $S(n) \propto n^{\mu}$, well-approximated by $\mu_{vw} = 0.52$ in the virtual world (Fig. 2 G), and by $\mu_{ethereum} = 0.61$ and $\mu_{polygon} = 0.52$

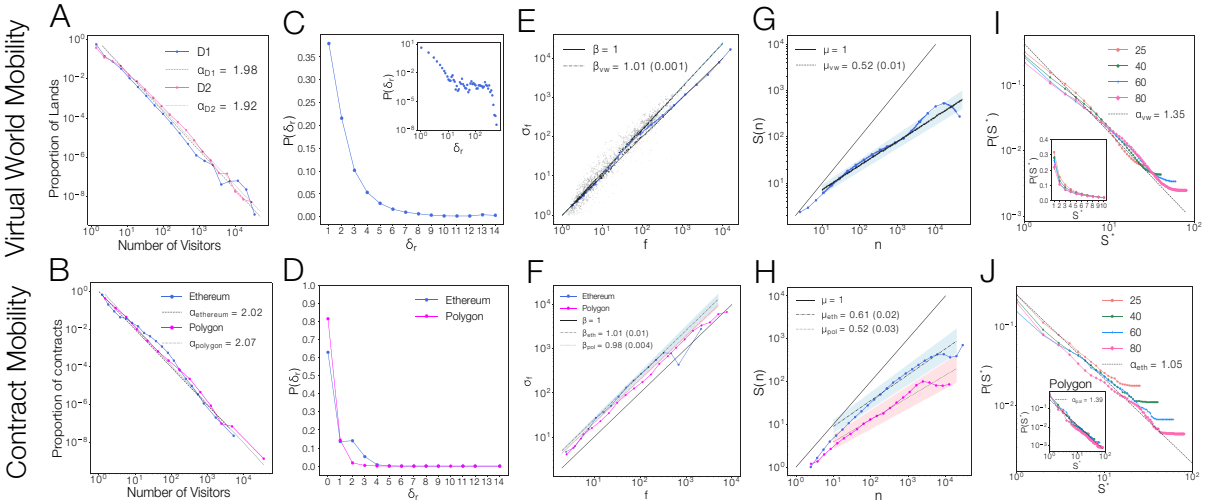

Fig. 2. Individual mobility patterns. **(A)** Distribution of number of visitors in the virtual world. We find that the proportion of visitors to different locations (lands) can be well-approximated by $P(S) \propto S^{-\alpha}$, where $\alpha_{D1} = 1.98$ and $\alpha_{D2} = 1.92$. **(B)** Distribution of number of users per node of the network. We find a fat-tailed distribution in number of visitors by contract, well-approximated by the power law exponent $\alpha_{Ethereum} = 2.02$ and $\alpha_{Polygon} = 2.07$. **(C)** Distance travelled in each displacement. We measure the jump distance, δ_r, as the Manhattan distance between two parcels. We find that individuals rarely move past a distance of 10. **(D)** Contract jump distance. We calculate jump distance, δ_r, as the shortest path length between two contracts in the network. A distance of $\delta_r = 0$ indicates purchase of a new NFT from the same contract. We find that the majority of the jumps occur in short distances, irrespective of the blockchain. Time allocation at different **(E)** lands and **(F)** contracts. We compare the mean visitation frequency $f_i = n/S$, where *n* is the total time spent and *S* is the number of locations, to the dispersion in visitation counts across all locations, σ_f. We find that $\sigma_f \propto f^{\beta}$, following $\beta_{vw} = 1.01$ in the virtual world, and $\beta_{ethereum} = 1.01$; $\beta_{polygon} = 0.98$ in the network space. As $\beta \sim 1$ it suggests that as individuals explore more, they tend to unevenly distribute their time across all locations. Number of unique locations visited over time. We measure the number of unique locations visited (*S*(*n*)) as a function of number of steps taken (*n*). We find that $S(n) \propto n^{\mu}$ scales as **(G)**$\mu_{vw} = 0.52$ in the virtual world and **(H)**$\mu_{ethereum} = 0.61$, $\mu_{polygon} = 0.52$ in the network space. These insights reveal a sub-linear scaling in the exploration new locations, suggesting that an individuals' inclination to visit more land decreases over time. **(I)** Location preference and time spent. We rank the locations visited based on the total number of visits to those locations, and display the proportion of time spent at each ranked location in the virtual world. This relationship is well-approximated using a power law with exponent $\alpha_{vw} = 1.35$. Inset shows the same plot in the linear scale. **(J)** Proportion of NFTs purchased from different contracts. Main panel shows the ranked frequency of locations based on the Ethereum blockchain, and the inset shows the results based on the Polygon blockchain. In both systems, the distribution of preference is well-approximated using a power law ($\alpha_{ethereum} = 1.05$, $\alpha_{polygon} = 1.39$).

in the contract space (Fig. 2 H). This sub linear scaling suggests that as individuals move in the virtual space or purchase from more contracts, the tendency to visit new locations decreases.

Finally, we ranked each location (land and contract) based on the number of times an individuals visited the location, so that $S^* = 3$ represents the third-most-visited location for the selected individual. We find that the probability of an individual returning to a specific location follows a power law, $P(S^*) \propto S^{-\alpha}$, characterized as $\alpha_{vw} = 1.1$ in the virtual world (Fig. 2 I) and $\alpha_{ethereum} = 1.01$ and $\alpha_{polygon} = 1.8$ (Fig. 2 J). That is, irrespective of the number of visited locations, individuals spend more than 50% of their time in three to five locations and tend to return to previously visited locations 90% of the time (Supplementary Figs. S15, S16), a pattern also characterizing mobility in the physical world[9].

Emergence of collective attention

The globalization of transportation has increased interest in selected spots around the world. For example, the Central Park in New York City, once a local park, now attracts an influx of visitors from all over the world[42]. To test whether patterns of high visitation emerge in the metaverse, which lacks traditional transportation systems and travel restrictions, we examine the total number of users that visit a specific location. We find that 76% (69,433) of the lands received at least one visitor, and there was substantial variation in visitation numbers across these visited locations: 21% (15,193) received a single visitor, 14% (9,391) were visited by two visitors, and the remaining 65% (44,849) received visits by three or more individuals (Supplementary Fig. S2).

Similarly, on the Ethereum blockchain, 31% (7,524) contracts received only one visitor, 14% (3,379) received two visitors, and the remaining 54% (12,924) received three of more visitors. Overall, in the virtual world, the top 1% of the lands attracted 94% of all visitors, while on the Ethereum blockchain, the top 1% of the contracts attracted 77% of the users, and on the Polygon blockchain, the top 1% of the contracts attract 96% of all users, a rather remarkable concentration of visits. We note that similarly pronounced differences in visitation patterns may also emerge in the physical space, such as within towns and cities.

To further quantify these patterns, we measured the distribution of the number of visitors to a land or contract (S), finding that it is well-approximated by the power law, $P(S) \propto S^{-\alpha}$, where the visitation exponent α in the virtual world is $\alpha_{D1} = 1.98$, and $\alpha_{D2} = 1.92$ (Fig. 2 A), and in the contract mobility space $\alpha_{ethereum} = 2.02$ and $\alpha_{polygon} = 2.07$ (Fig. 2 B). We find the distributions to be stable over time (Supplementary Fig. S3), indicating that in the metaverse a few lands and contracts consistently attract most of the users while most locations struggle to find visitors.

The ability of a location to attract traffic could potentially elevate the prices of the lands or property[43]. Somewhat surprisingly, we find that the selling price of a land in metaverse is not correlated with the number of visitors it receives ($\beta = 0.002$, CI:[−0.02, 0.02], Supplementary Fig. S6). For example, the land at location (118,−10) attracted 196 visitors and fetched a selling price of $4,029, while a nearby land (120,−12) attracted 2,053 visitors but was sold only $3,566 (Supplementary Fig. S7). In other words, despite receiving an order of magnitude more visitors compared to (118,−10), land (120,−12) was unable to demand a higher valuation, indicating that the virtual world does not create inflationary prices depending on the number of visitors.

Further, urban centers, representing geographical clusters that attract high number of visitors, illustrate the significance of geographical proximity in land visitation patterns[44]. In the virtual world, we discover the emergence of local neighborhoods characterized by high visitation, mirroring patterns observed in the physical world (Supplementary Fig. S8 A). However, in the metaverse land prices are not geographically clustered ($\beta = 0.294$, CI:[0.27, 0.31], $R^2 = 0.1$, Supplementary Fig. S9). That is, proximity to popular locations is not a strong determinant of land prices (Supplementary Section 2), indicating that distance and amenities do not determine the sale price of locations. This lack of a correlation between land prices and visitation underscores the distinctive feature of the metaverse, where economic and spatial mobility dynamics offer room for new urban development theories[45,46].

In summary, our empirical observations reveal a pronounced disparity in visitor distribution across various locations within the metaverse. The spatial layout of locations in the virtual world leads to the emergence of clusters of high visitation, revealing high similarities to the emergence of hotspots in the real-world. Some of these features may be influenced by the design choices of Decentraland, like the grid-like map that limits any location from having more than 8 spatial neighbors. Hence, further work is needed to generalize our findings to other virtual worlds, such as Second Life, that employ different design and game mechanics.

Macroscopic patterns of mobility networks

As illustrated in Fig. 2, although these two systems within the metaverse - a virtual world with an imposed 2D structure and blockchain-based NFT contracts forming an infinite dimensional network– are fundamentally distinct, they nertheless display a striking quantitative similarity in individual mobility patterns. This prompts us to ask, do the individual decisions driving these patterns are also driven by similar mechanisms, resulting in similar large-scale mobility patterns? To address this question, we develop a common network framework that captures mobility in both systems (Supplementary Section 4): (a) the virtual world network (VWN), where a node indicates a land (locations) and a link signifies temporal movement between the two lands. (b) the contract network (CN), where a node indicates a contract (location) and a link captures temporal movement between the two contracts.

We find that the degree distribution of nodes in both mobility networks have a heavy tail, where the probability of finding a location with degree k scales as $P(k) \propto k^{-\alpha}$. In the virtual world network we find $\alpha_{vw} = 1.98$ (Fig. 4 A), while in contract networks we find $\alpha_{ethereum} = 2.9$ and $\alpha_{polygon} = 2.4$ (Fig. 4 B). The fact that $2 \lesssim \alpha < 3$ in Ethereum and Polygon contract networks, resulting in the divergence of $\langle k^2 \rangle$, indicates that a few hub locations receive a disproportionate number of connections[47–49].

To assess movement between locations, we examine the number of individuals traveling between two locations, quantified via the link weight, w_{ij}. We find that in both mobility networks the link weight distributions follows a power law, $P(w_{ij}) \propto w_{ij}^{-\alpha}$, well-approximated by $\alpha_{vw} = 2.07$ in the virtual world network (Fig. 4 D) and $\alpha_{ethereum} = 2.85$ and $\alpha_{polygon} = 2.5$ in the contract network (Fig. 4 E). That is, if individuals moved randomly between locations, we would fail to observe such concentrated movement within a few specific locations (Supplementary Section 4.1).

Finally, we find that a location's degree centrality within the network influences the number of individuals visiting that location: the number of visitors to a location follows $N_S \propto k^{\beta}$, where in the virtual world network we have $\beta_{vw} = 1.05$ (Fig. 4 G), and in the contract network $\beta_{ethereum} = 1.05$ and $\beta_{polygon} = 1.13$ (Fig. 4 H). This pattern remains consistent when examining the connection between centrality of the contract and the number of NFTs sold (Supplementary Fig. S17). The fact that $\beta \sim 1$ suggests that locations central within the meta-mobility network experience a linearly higher increase in the number of visitors compared to locations with fewer connections.

Modeling the origins of metaverse mobility

Our empirical results underscore four aspects of human mobility, each captured by a distinct scaling law: (1) individuals exhibit sub linear exploration patterns ($S(n) \propto n^{\mu}$ as $\mu < 1$), (2) The frequency of visits to all locations follows a power law distribution ($P(S^*) \propto S^{-\alpha}$ as $1 < \alpha < 2$), and (3) the movement between the various locations defines a mobility network that exhibits a power law degree distribution ($P(k) \propto k^{-\alpha}$ with $2 < \alpha < 3$), and (4) the flow between locations (link weights) follows another power law distribution ($P(w_{ij}) \propto w_{ij}^{-\alpha}$ with $2 < \alpha < 3$).

To understand how well the existing models can account for mobility in the metaverse, we start from the Exploration and Preferential Return (*EPR*) model[50], which has emerged as a foundational framework for understanding human mobility in the physical world[26,40,51,52]. In the model, at each time step an individual decides to move to a randomly chosen new location based on the probability $p_{new} = \rho S^{-\gamma}$, where S is the number of previously visited locations, or returns to a previously visited location based on their past visitation history with probability $1 - p_{new}$ (Supplementary Section 5). Previous studies have estimated $\gamma_{EPR} = 0.21$ in the physical world[50], different from $\gamma_{vw} = 0.41 \pm 0.03$ we observe in the virtual world, and the values $\gamma_{ethereum} = 0.07 \pm 0.01$ and $\gamma_{polygon} = 0.18 \pm 0.01$ we observe in the contract space (Supplementary Fig. S19 A-C). This implies that contract mobility, defined by $\gamma_{ethereum}$ and $\gamma_{polygon}$, experiences a slower decay rate in exploration compared to the physical world, showing a higher propensity to keep exploring new locations. On the other hand, the virtual world exhibits a faster decay rate (high γ_{vw}) compared to the physical world or the contract space, suggesting that individuals are less likely to explore new virtual locations[53].

The *EPR* model predicts the individual visitation frequency of locations, $P(S^*) \propto S^{-\alpha_{EPR}}$, with exponent $\alpha_{EPR} = 1.42 \pm 0.03$, together with a sub-linear exploration patterns in new visitation, $S \propto n^{\mu_{EPR}}$, as $\mu_{EPR} = 0.7 \pm 0.01$ (Table S1, Supplementary Section 5.4). This shows that the *EPR* model is able to account for the observed sub-linear visitation patterns and the power law distribution in visited locations ($\alpha_{vw} = 1.35 \pm 0.03$, $\mu_{vw} = 0.52 \pm 0.01$), as highlighted in key observations (1) and (2).

Yet, as the agents select locations randomly, the *EPR* model is unable to uncover the emergence of visitation hubs and the network-based relationship between the locations as documented in Fig. 4, i.e., the patterns (3) and (4). In particular, the network structure predicted by the *EPR* model is not scale-free (Fig. 4 C), violating observation (3). It also fails to predict heterogeneous visitation patterns, i.e. observation (4), finding link weights that are several magnitudes lower than empirical data, and fails to capture the linear correlation between hubs and their visitation numbers (Fig. 4 F, I). In fact, the mobility networks generated by the EPR model closely resembles random movements without preferential return (Supplementary Fig. S18), suggesting that the model offers inadequate explanations about collective mobility, as highlighted in observations (3) and (4).

To resolve this discrepancy, we extend the *EPR* model by incorporating the relative popularity of each location, biasing the individual movements towards more popular locations, and removing the limitation of movements based on distance (Supplementary Section 5.3). In this new metaverse-adopted EPR model, that we call the *m-EPR* model (Fig. 3), an individual decides to move to a new location with probability $p_{new} = \rho S^{-\gamma}$, or return to a previously visited location with probability $1 - p_{new}$, mirroring the *EPR* model. Yet, in both scenarios we add a new element: before making a move, an individual evaluates the popularity of all available locations, and moves according to the transition probability, $\pi_j = m_j / \sum_i m_i$, where m_j is the number of visits to location j by all agents. Unlike the *EPR* model and its several proposed variants[18,26,40,51,52,54], the *m-EPR* model informs the individual movement based on the location's visitation numbers, normalized across all locations irrespective of distance. Since the mobility costs are diminished in the metaverse, the *m-EPR* model does not adjust transition probability based on the distance between locations, making it a more flexible framework for capturing metaverse mobility patterns compared to previous models. Indeed, the empirical data indicates that an individual is significantly more inclined to visit a location with higher visitation numbers compared to those with fewer visitation numbers ($\beta = 0.95$, $R^2 = 0.88$), offering the empirical rationale for the added component (Supplementary Fig. S19 D-F).

To explore the predictive power of the proposed *m-EPR* model, we performed simulations using parameters derived from the virtual world ($\gamma_{vw} = 0.41$), and explored the model-based predictions by determining the scaling exponents related to individual mobility and the mobility network (Table S1). We also examined simulations with different temporal and spatial parameters (Supplementary Figs. S20, S21). In each case, we find a remarkable alignment with the empirical observations.

To be specific, we find that the *m-EPR* model recreates the individual mobility patterns (key observations (1) and (2)), by predicting a sub linear behavior in exploration, $S \propto n^{\mu_M}$ with $\mu_M = 0.6 \pm 0.004$, closely related to the empirically observed values of $\mu_{vw} = 0.52 \pm 0.01$ (Supplementary Fig. S22 A). The model also

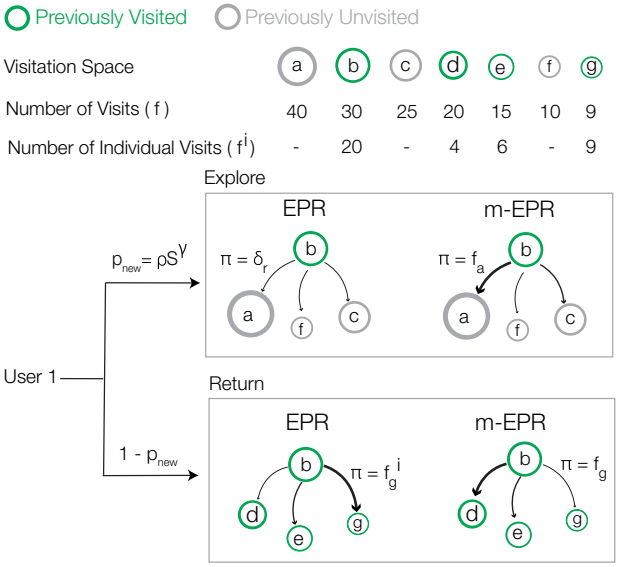

Fig. 3. Foundation of the mobility model. We first organize the possible visiting locations *a* to *g*, into whether the location has been previously visited (green) or unvisited (gray). At each movement, an individual decides to explore a new location (gray) with probability $p_{new} \propto S^{-\gamma}$, where S represents the number of previously visited locations. With its complementary probability, $1 - p_{new}$, an individual decides to revisit a previously visited location (green). In the EPR formulation, when visiting a new location, the individual randomly selects a new location drawn at some distance δ_r. In the proposed *m-EPR* model, the individual is biased towards the more popular locations, sampled according to the probability $\pi = m_a / \sum_j m_j$, where m_a is the popularity of the location *a*. When deciding to revisit a previously visited location, in the *EPR* model the individual selects based on their individual past visitation history, $\pi_i = m_g^i / \sum_j m_j^i$, where m_g^i represents the number of visits to the location *g* by individual *i*. In contrast, in the *m-EPR* model, an individual revisits a location according to the probability $\pi = m_g / \sum_j m_j$, where m_g represents the total number of visits to the location *i* by all individuals. In contrast to the EPR model, where an individual randomly selects a new location and preferentially re-visits location based on only their individual visitation history (π_i), the *m-EPR* model allows individuals to select new locations and revisit old locations based on their global popularity (π).

identifies a power law visitation frequency distribution, $P(S^*) \propto S^{-\alpha_M}$, where $\alpha_M = 1.41 \pm 0.02$, consistent with empirical observations of $\alpha_{vw} = 1.35 \pm 0.03$ (Supplementary Fig. S22 B).

Importantly, the *m-EPR* model can successfully capture the emergent characteristics of the observed mobility network (key observations (3) and (4)). Specifically, we observe that the *m-EPR* model predicts a scale-free network with degree distribution, $P(k) \propto k^{-\alpha_M}$, with $\alpha_M = 2.1 \pm 0.06$ (Fig. 4 C), closely aligned with empirical observations ($\alpha_{vw} = 1.98 \pm 0.01$). Further, the *m-EPR* model accurately captures the link weight distribution, $P(w_{ij}) \propto w_{ij}^{\alpha_M}$, with exponent $\alpha_M = 2.19 \pm 0.03$ (Fig. 4 F), suggesting that the model explains the visitation heterogeneity that emerges in the mobility network ($\alpha_{vw} = 2.18 \pm 0.08$). Finally, the *m-EPR* model, by encouraging individual movements to popular locations, successfully captures the positive relationship between a location's degree and the number of visitors, $N(S) \propto k^{\beta_M}$, where $\beta_M = 0.96 \pm 0.03$ (Fig. 4 I), consistent with $\beta_{vw} = 1.05 \pm 0.002$) found in the empirical data.

Indeed, the *EPR* model, which assumes that individuals select their new locations independently of each other, overlooks the interconnected dynamics of exploration. Since *EPR* and related models are designed to account for spatial and temporal constraints imposed by residence, workplace, travel time and cost, they neglect the influence of popularity. As a result, they are unable to capture the heterogeneous flows observed between locations in the metaverse. In contrast, the *m-EPR* predicts mobility network and heterogeneous mobility flows, and captures the essential features of virtual mobility. The ability of the *m-EPR* model to accurately describe the aggregate level patterns of the mobility network implies that popularity is a strong determinant of individual movement in the metaverse.

Discussion

The metaverse represents experiences, identities, and digital assets that help create a novel creator economy, resulting in networks that capture the underlying individual interactions, facilitated using blockchain technology. Importantly, the metaverse offers a freedom of mobility, releasing individuals from the traditional constraints imposed by mobility costs[36]. In theory, this newfound freedom of movement offers the potential for a more equitable distribution of access and human activity patterns[55]. Yet, by analyzing large scale data on human movements in the virtual world and purchasing of new NFTs, we find that the exploration patterns of individuals

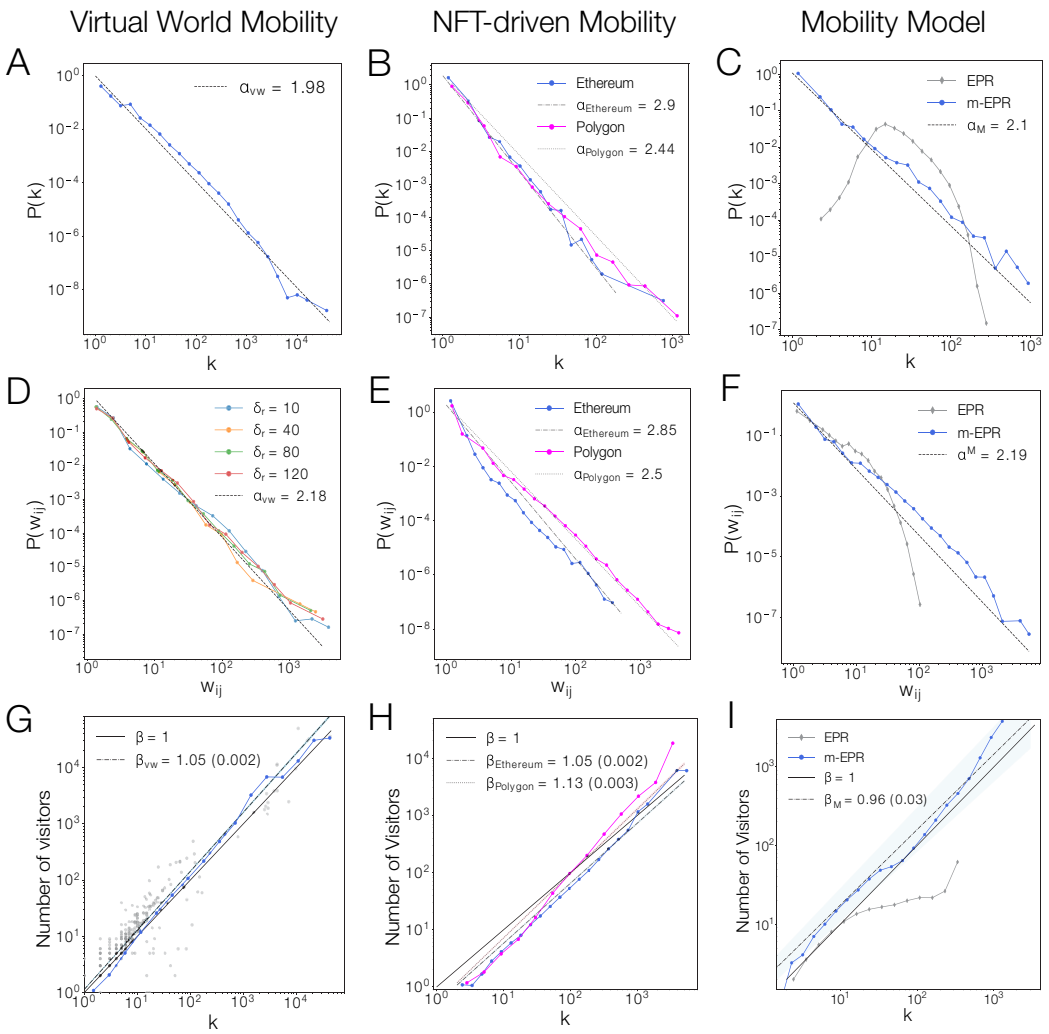

Fig. 4. Capturing models of meta-mobility. **(A)** Degree distribution of lands in the mobility network. We observe a fat tailed distribution in degrees, well-approximated by a power law, $P(k) \propto k^{-\alpha}$ as $\alpha_{vw} = 1.98$. **(B)** Degree distribution of contracts in the contract network. We observe a heavy tailed distribution where few contracts receive most of the connections, well-approximated by a power law, $P(k) \propto k^{-\alpha}$, where $\alpha_{ethereum} = 2.9$ and $\alpha_{polygon} = 2.4$. **(C)** Degree distribution from the model simulations. We show the results from the EPR model and the m-EPR model, finding that the m-EPR model recreates the heterogeneous degree distribution as $\alpha^M = 2.1 \pm 0.06$. We show the link weight, w_{ij}, distribution of the network for **(D)** virtual world mobility and **(E)** contract mobility. The link weight distribution follows a power law decay as $P(w_j) \propto w_{ij}^{-\alpha}$, where $\alpha_{vw} = 2.18$ in the virtual world and $\alpha_{ethereum} = 2.85$; $\alpha_{polygon} = 2.5$ in the contract network. We display link weight distributions between nodes at different physical distances (δ_r). **(F)** Link weight distribution from model simulations. We find that the m-EPR model is able to uncover the concentrated flows between locations with $\alpha^M = 2.19 \pm 0.03$ in the network. **(G)** Relationship between degree of land in the virtual world mobility network and its number of visitors. We find that the two variables scales as $N_S \propto k^{\beta}$, where $\beta_{vw} = 1.05$. **(H)** Relationship between degree of contract in the contract mobility network and its number of visitors. We find that $N \propto k^{\beta}$, where $\beta_{ethereum} = 1.05$ and $\beta_{polygon} = 1.13$. **(I)** Relationship between degree and visitors from model simulations. We find that the*m-EPR* model obtains a positive scaling between the two variables ($\beta^M = 0.96 \pm 0.03$).

results in highly uneven number of visitations across different locations. These empirical findings prompted us to modify the existing human mobility models so that we can adapt them to the metaverse environment. The resulting *m-EPR* model leverages a popularity-driven mechanism to successfully replicate individual level characteristics and the aggregate mobility patterns in both the virtual world and the contract space. The model's ability to explain the observed quantitative patterns is rooted in a simple prospective mechanism: an individual's inclination to visit a specific location is influenced by the number of previous visitors to that location, irrespective of his/her own visitation history or distances between locations. This mechanism, absent from mobility in the physical world, fundamentally alters the quantitative patterns of metaverse mobility.

At the same time, individual movements in the metaverse preserves multiple properties observed in the physical world. For example, an individual's inclination to explore new locations diminishes over time, and individuals display substantial heterogeneity in visitation preference across all visited locations. These consistent patterns underscore the persistent elements of human movements, holding relevance in both physical and metaverse environments. Further, the quantitative insights gained by studying human behavior patterns through public blockchain data could help formulate new theories of human attention in the virtual spaces[56].

Note that virtual worlds also contain a three-dimensional component[57]. For example, individuals could hike a mountain or hang out at the top of a building, dimensions captured by the data we collected and available for future work. The current modeling framework overlooks these extra dimensions, along with other features that influence human decisions in mobility, such as the impact of social networks on location choices, the different utility or aesthetic appeal of the available locations, and the potential activities within specific points of interest–such as playing poker at a virtual casino[58], or viewing digital art at Sotheby's virtual gallery[59]. Future work should address their role in predicting sale prices of locations, and may also design controlled experiments to understand the value of autonomous generative agents in enabling social interactions and location discovery[60].

Methods

Constructing meta-mobility systems

Virtual world mobility. The data regarding the movements of individuals is derived from Decentraland, one of the first decentralized virtual worlds. We conduct two data collection processes (Supplementary Section 1). First data collection process lasted from March 15, 2022 to Aug 6, 2022, extracting data from a single data server, resulting in 81,563 users and 110,416,682 displacements (D1), and the second data collection lasted from Aug 7,2022 to September 19, 2022, capturing 141,226,580 movements by 94,149 users and (D2). Finally, we collect 15,209 sales of 6,773 lands, and 1,562 sales of 1,075 estates (collection of land) comprising of 7,159 lands. In the mobility network, a node is a land and a link signifies movement between the two locations. We create the mobility network by aggregating the movements of all individuals (Fig. 1 A, Supplementary Section 1.1).

Contract network mobility. Each NFT is associated with a specific contract, either of type ERC-721 or ERC-1155, representing transaction rules and royalty rates for each NFT transfer. An individual follows the rules set by the contract to purchase an NFT, similar to how collectors purchase an art item (NFT) from an art gallery (contract). For the same set of individuals, whose wallets we followed on Decentraland, we extract data regarding NFT purchases from two different blockchains: (a) Ethereum, finding 1,165,310 NFTs from 23,827 contracts collected by 14,732 (9%) users, and (b) Polygon, find 3,112,300 NFTs from 54,918 contracts by 41,870 (25%) users. Using the NFT purchase history of each individual, we build a contract network, where a NFT contract for *Foundation* will be connected to another NFT contract for *Artblocks*, if an individual purchased a NFT from *Foundation* and then subsequently purchased an NFT from *Artblocks* (Fig. 1 A). The resulting contract network captures similarities between contracts and also characterises mobility in the NFT space (Fig. 1 C, Supplementary Section 1.3).

Modelling metaverse mobility

EPR model. The simulations are conducted on a 300x300 location grid, and the choice of the location is sampled from the jump distribution derived from empirical data. The probability that an individual chooses to explore a new location is given by $p_{new} \propto S^{-\gamma}$, where S is the number of locations visited by the individual so far. With probability, $1 - p_{new}$, the individual decides to revisit a previously visited location, proportional to the number of past visits.

m-EPR model. The individual decides to explore a new location with probability $p_{new} \propto S^{-\gamma}$, and with probability $1 - p_{new}$, the revisit a previously visited location. In contrast to the *EPR* model, the individual movements are influenced by the popularity of each location, characterized by the number of visits to that location, $\pi = m_g / \sum_j m_j$, where m_g represents the total number of visits to the location *i* by all individuals. To do this, we keep track of the number of visitors, $m_t(i)$ to a location *i*. At the end of each time step, the number of visitors to the location, $m_{t+1}i$ is updated.

Simulation strategy. The simulations were conducted for $n = 5,000$ agents and $S = 20,000$ locations in a infinite dimensional space, meaning the distance between locations does not affect the transition probability. At time $t = 0$, the *n* agents are randomly distributed to *S* locations. At each time step, an agent becomes active proportional to their activity level drawn from the empirical distribution, and make $m = 4$ movements (the number of steps is arbitrary and does not influence the macroscopic patterns). The agent visits a new location with probability p_{new} and with probability $1 - p_{new}$ they revisit a previously visited location. The choice of the location is decided based on the number of visits by all agents, and the transition probabilities between locations are updated following each individual's trajectory. The trajectories were simulated until the visitation patterns achieved a stationary condition (n Section 5). The simulations followed discrete time movement, and it does not incur any waiting time prior to each movement.

Data availability

The code required to get the latest mobility data in both web3 systems, along with tools to recreate the analysis, is provided at https://github.com/Barabasi-Lab/metaverse-mobility. An overview of the virtual world data can be found at https://www.dcl-metrics.com/. The entire data set used in this study can be on Zenodo at https://zenodo.org/records/14852203.

Received: 1 August 2025; Accepted: 17 March 2026
Published online: 04 April 2026

References

1. Caldarelli, G. et al. The role of complexity for digital twins of cities. *Nat. Comput. Sci.* https://doi.org/10.1038/s43588-023-00431-4 (2023).
2. M. Ball, The metaverse: and how it will revolutionize everything (Liveright Publishing, 2022).
3. Marthews, A. & Tucker, C. E. *Blockchain and Identity Persistence* (Legal and Monetary Perspectives, 2019).
4. E. G. Weyl, P. Ohlhaver & V. Buterin, Decentralized society: Finding Web3's soul, Available at SSRN 4105763 (2022).
5. Vasan, K., Janosov, M. & Barabási, A.-L. Quantifying NFT-driven networks in crypto art. *Sci. Rep.* **12**, 1 (2022).
6. Nadini, M. et al. Mapping the NFT revolution: Market trends, trade networks, and visual features. *Sci. Rep.* **11**, 20902 (2021).
7. Huynh-The, T. et al. Blockchain for the metaverse: A review. *Future Gener. Comput. Syst.* **143**, 401 (2023).
8. Mckinsey, Value creation in the metaverse, https://www.mckinsey.com/capabilities/growth-marketing-and-sales/our-insights/value-creation-in-the-metaverse (2022).
9. Gonzalez, M. C., Hidalgo, C. A. & Barabasi, A.-L. Understanding individual human mobility patterns. *Nature* **453**, 779 (2008).
10. J. Yuan, Y. Zheng & X. Xie, Discovering regions of different functions in a city using human mobility and POIs, *Proceedings of the 18th ACM SIGKDD international conference on Knowledge discovery and data mining*, 186–194 (2012)
11. Zhao, C., Zeng, A. & Yeung, C. H. Characteristics of human mobility patterns revealed by high-frequency cell-phone position data. *EPJ Data Sci.* **10**, 5 (2021).
12. Simini, F., González, M. C., Maritan, A. & Barabási, A.-L. A universal model for mobility and migration patterns. *Nature* **484**, 96 (2012).
13. Crandall, D. J. et al. Inferring social ties from geographic coincidences. *Proc. Natl. Acad. Sci. U. S. A.* **107**, 22436 (2010).
14. Eagle, N., Macy, M. & Claxton, R. Network diversity and economic development. *Science* **328**, 1029 (2010).
15. Davis, A., Murphy, J., Owens, D., Khazanchi, D. & Zigurs, I. Avatars, people, and virtual worlds: Foundations for research in metaverses. *J. Assoc. Inf. Syst.* https://doi.org/10.17705/1jais.00183 (2009).
16. Echenique, F. & Fryer, R. G. Jr. A measure of segregation based on social interactions. *Q. J. Econ.* **122**, 441 (2007).
17. Netto, V. M., Soares, M. P. & Paschoalino, R. Segregated networks in the city. *Int. J. Urban Reg. Res.* **39**, 1084 (2015).
18. Moro, E., Calacci, D., Dong, X. & Pentland, A. Mobility patterns are associated with experienced income segregation in large US cities. *Nat. Commun.* **12**, 4633 (2021).
19. Napoli, L., Sekara, V., García-Herranz, M. & Karsai, M. Socioeconomic reorganization of communication and mobility networks in response to external shocks. *Proc. Natl. Acad. Sci. U. S. A.* **120**, e2305285120 (2023).
20. Bonaccorsi, G. et al. Economic and social consequences of human mobility restrictions under COVID-19. *Proc. Natl. Acad. Sci. U. S. A.* **117**, 15530 (2020).
21. Kojaku, S., Hébert-Dufresne, L., Mones, E., Lehmann, S. & Ahn, Y.-Y. The effectiveness of backward contact tracing in networks. *Nat. Phys.* **17**, 652 (2021).
22. Chang, S. et al. Mobility network models of COVID-19 explain inequities and inform reopening. *Nature* **589**, 82 (2021).
23. Santana, C. et al. COVID-19 is linked to changes in the time-space dimension of human mobility. *Nat. Hum. Behav.* **7**, 1729 (2023).
24. Hazarie, S., Barbosa, H., Frank, A., Menezes, R. & Ghoshal, G. Uncovering the differences and similarities between physical and virtual mobility. *J. R. Soc. Interface* **17**, 20200250 (2020).
25. Zhong, C. et al. Revealing centrality in the spatial structure of cities from human activity patterns. *Urban Stud.* **54**, 437 (2017).
26. Yan, X.-Y., Wang, W.-X., Gao, Z.-Y. & Lai, Y.-C. Universal model of individual and population mobility on diverse spatial scales. *Nat. Commun.* **8**, 1639 (2017).
27. Radicchi, F., Baronchelli, A. & Amaral, L. A. Rationality, irrationality and escalating behavior in lowest unique bid auctions. *PLoS One* **7**, e29910 (2012).
28. Szell, M., Sinatra, R., Petri, G., Thurner, S. & Latora, V. Understanding mobility in a social petri dish. *Sci. Rep.* **2**, 1 (2012).
29. Szell, M. & Thurner, S. Social dynamics in a large-scale online game. *Adv. Complex Syst.* **15**, 1250064 (2012).
30. B. Guidi & A. Michienzi, The social impact of NFTs in the metaverse economy, *Proceedings of the 2023 ACM Conference on Information Technology for Social Good*, 428–436 (2023).
31. J. Luo, S. Casale-Brunet, B. Guidi, M. Mattavelli & X. Liu, Unveiling social aggregation in the Decentraland metaverse platform, *Proceedings of the 2023 ACM Conference on Information Technology for Social Good* , 419–427 (2023).
32. T. Hu, J. Luo & W. Liu, Life in the Matrix: Human Mobility Patterns in the Cyber Space, *Proceedings of the International AAAI Conference on Web and Social Media*, **12**, (2018).
33. T. Hu, Y. Xia & J. Luo, To return or to explore: Modelling human mobility and dynamics in cyberspace, *The World Wide Web Conference*, 705–716 (2019).
34. Barbosa, H. et al. Human mobility: Models and applications. *Phys. Rep.* **734**, 1 (2018).
35. Sinatra, R. & Szell, M. Entropy and the predictability of online life. *Entropy* **16**, 543 (2014).
36. Bainbridge, W. S. The scientific research potential of virtual worlds. *Science* **317**, 472 (2007).
37. Finck, M. Blockchains and data protection in the European Union. *Eur. Data Prot. L. Rev.* **4**, 17 (2018).
38. Alessandretti, L., Aslak, U. & Lehmann, S. The scales of human mobility. *Nature* **587**, 402 (2020).
39. Bokányi, E., Juhász, S., Karsai, M. & Lengyel, B. Universal patterns of long-distance commuting and social assortativity in cities. *Sci. Rep.* **11**, 1 (2021).
40. Schläpfer, M. et al. The universal visitation law of human mobility. *Nature* **593**, 522 (2021).
41. E. Adar, J. Teevan & S. T. Dumais, Large scale analysis of web revisitation patterns, *Proceedings of the SIGCHI conference on Human Factors in Computing Systems*, 1197–1206 (2008).
42. Bertaud, A. Order without design: How markets shape cities. *Town and Regional Planning* **79**, 2 (2021).
43. Zukin, S. et al. New retail capital and neighborhood change: Boutiques and gentrification in New York City. *City Community* **8**, 47 (2009).
44. S. Hasan, X. Zhan & S. V. Ukkusuri, Understanding urban human activity and mobility patterns using large-scale location-based data from online social media, *Proceedings of the 2nd ACM SIGKDD international workshop on urban computing* 1–8 (2013).
45. G. West, Scale: The universal laws of life, growth, and death in organisms, cities, and companies (Penguin, 2018).
46. Hong, I., Frank, M. R., Rahwan, I., Jung, W.-S. & Youn, H. The universal pathway to innovative urban economies. *Sci. Adv.* **6**, eaba4934 (2020).
47. Barabási, A.-L. & Albert, R. Emergence of scaling in random networks. *Science* **286**, 509 (1999).
48. Albert, R. & Barabási, A.-L. Statistical mechanics of complex networks. *Rev. Mod. Phys.* **74**, 47 (2002).
49. Barrat, A., Barthelemy, M., Pastor-Satorras, R. & Vespignani, A. The architecture of complex weighted networks. *Proc. Natl. Acad. Sci. U. S. A.* **101**, 3747 (2004).
50. Song, C., Koren, T., Wang, P. & Barabási, A.-L. Modelling the scaling properties of human mobility. *Nat. Phys.* **6**, 818 (2010).
51. Ren, Y., Ercsey-Ravasz, M., Wang, P., González, M. C. & Toroczkai, Z. Predicting commuter flows in spatial networks using a radiation model based on temporal ranges. *Nat. Commun.* **5**, 5347 (2014).
52. Pappalardo, L., Manley, E., Sekara, V. & Alessandretti, L. Future directions in human mobility science. *Nat. Comput. Sci.* **3**, 1 (2023).
53. Eisenbeiss, M., Blechschmidt, B., Backhaus, K. & Freund, P. A. The (real) world is not enough: Motivational drivers and user behavior in virtual worlds. *J. Interact. Mark.* https://doi.org/10.1016/j.intmar.2011.06.002 (2012).
54. Pappalardo, L., Rinzivillo, S. & Simini, F. Human mobility modelling: Exploration and preferential return meet the gravity model. *Procedia Comput. Sci.* **83**, 934 (2016).

55. Mazalek, A., Chandrasekharan, S., Nitsche, M., Welsh, T. & Clifton, P. *Reinventing ourselves: contemporary concepts of identity in virtual worlds* 129–151 (Springer, 2011).
56. Lazer, D. Studying human attention on the Internet. *Proc. Natl. Acad. Sci. U. S. A.* **117**, 21 (2020).
57. J. D. N. Dionisio W. G. B. Iii & R. Gilbert, 3D virtual worlds and the metaverse: Current status and future possibilities, ACM Computing Surveys (CSUR) **45**, 1 (2013).
58. C. D'Anastasio, Sotheby's opens a virtual gallery in decentraland, https://www.bloomberg.com/news/articles/2022-03-01/what-is-decentraland-metaverse-is-often-used-for-crypto-poker (2022).
59. Decentraland, Sotheby's opens a virtual gallery in decentraland, https://decentraland.org/blog/announcements/sotheby-s-opens-a-virtual-gallery-in-decentraland (2021).
60. J. S. Park, et al., Generative agents: Interactive simulacra of human behavior, *Proceedings of the 36th Annual ACM Symposium on User Interface Software and Technology,* 1–22 (2023).

Acknowledgements
We thank the data providers of this study: Etherscan, a block explorer platform for Ethereum; Polygonscan, a block explorer for Polygon, and the Decentraland Foundation.

Author contributions
KV designed the experiments and conducted the analysis. All authors conceived and wrote the manuscript.

Funding
This work was supported by the Templeton Foundation under contract 61066, the Air Force Office of Scientific Research under award number FA9550-19-1-0354, and the Eric and Wendy Schmidt Fund for Strategic Innovation (G-22-63228), and the National Science Foundation (SES-2219575). ALB was also supported by European Research Council (ERC) Synergy grant (DYNASNET-810115). M.K. was supported by the Accelnet-Multinet NSF grant. M.K. acknowledges funding from the National Laboratory for Health Security (RRF-2.3.1-21-2022-00006); the SoBigData++ H2020-871042 project and the MOMA WWTF project.

Declarations

Competing interests
A.-L.B. is the founder of Scipher Medicine and Foodome, companies that explore the use of network-based tools in health. K.V and M.K do not report any competing interests.

Ethical approval
The project was granted Institutional Review Board (IRB) exemption by Northeastern University (Reference number 23-03-29).

Inclusion and diversity
We support inclusive, diverse, and equitable conduct of research.

Additional information
Supplementary Information The online version contains supplementary material available at https://doi.org/10.1038/s41598-026-45128-6.

Correspondence and requests for materials should be addressed to A.-L.B.

Reprints and permissions information is available at www.nature.com/reprints.

Publisher's note Springer Nature remains neutral with regard to jurisdictional claims in published maps and institutional affiliations.